Visualizing Evolutionary Activity of Genotypes

Mark A. Bedau
C. Titus Brown*
Reed College
3203 SE Woodstock Blvd.
Portland, OR 97202
{mab, brown}@reed.edu

Abstract We introduce a method for visualizing evolutionary activity of genotypes. Following a proposal of Bedau and Packard [11], we define a genotype's evolutionary activity in terms of the history of its concentration in the evolving population. To visualize this evolutionary activity we graph the distribution of evolutionary activity in the population of genotypes as a function of time. Adaptively significant genotypes trace a salient line or "wave" in these graphs. The quality of these waves indicates a variety of evolutionary phenomena, such as competitive exclusion, neutral variation, and random genetic drift. We apply this method in an evolutionary model of self-replicating assembly language programs competing for room in a two-dimensional space. Comparison with fitness graphs and with a nonadaptive analogue of this model shows how this method highlights adaptively significant events.

Keywords
adaptation, evolutionary activity, visualization, neutral variation, random genetic drift, genotypes

1 How to Visualize Evolutionary Activity

Although it is commonly accepted that the process of adaptation produces much of the order and functionality evident in complex systems [18, 19, 21, 22, 26], it is often difficult to distinguish adaptive change in a system from other evolutionary phenomena such as random genetic drift [15, 20, 27, 38]. The problem is not a shortage of data but the inability to highlight the *relevant* data. Those studying artificial models have the luxury of being able to collect virtually complete data; aside from storage space, only imagination limits what kinds of data are gathered. But this compounds rather than alleviates the problem of filtering this data to find a picture that reveals a system's significant adaptive phenomena. The study of evolutionary dynamics in natural and artificial systems dearly needs an effective method for visualizing adaptive phenomena.

We here introduce a method for visualizing adaptive phenomena involving genotypes, and we illustrate this method by applying it to the evolutionary dynamics generated by a simple model of evolving machine language programs. Our visualization method is a generalization of the way Bedau and Packard visualized and quantified what they called "evolutionary activity" [11]. Bedau and Packard focused on activity at the level of individual alleles, and they illustrated their visualization method only briefly. The primary novelties of the present article are to apply the approach at a new level of analysis—whole genotypes—and then to give detailed analyses of the adaptive phenomena revealed in a series of specific cases of evolution. These analyses disclose the characteristic signatures of a variety of evolutionary phenomena involving geno-

* Present address: MC 106-38, Computation and Neural Systems, California Institute of Technology, Pasadena, CA 91125; ctb@cns.caltech.edu

types, including competitive interactions among genotypes, clouds of neutral variant genotypes acting in concert, and random genetic drift among neutral variant genotypes.

The fundamental idea behind evolutionary activity of genotypes is to identify those genotypes that make a difference in the evolutionary process. Generally we consider a genotype to "make a difference" if it continues to be active in the evolving system. Here we measure evolutionary activity of genotypes in the context of the Evita model, a simple artificial system that consists of evolving assembly language programs competing for space, akin to Tierra [30]. In this model the relative adaptive significance of a genotype is reflected by its concentration in the population. Relatively well-adapted genotypes will have a relatively high concentration in the population, and relatively poorly adapted genotypes will be correspondingly scarce. Thus, we here define the *evolutionary activity* $a_i(t)$ of the ith genotype at time t as its concentration integrated over the time period from its origin up to t, provided it exists:

$$a_i(t) = \begin{cases} \int_0^t c_i(t)\, dt & \text{if genotype } i \text{ exists at } t \\ 0 & \text{otherwise,} \end{cases} \tag{1}$$

where $c_i(t)$ is the concentration of the ith genotype at t, that is, the fraction of the population that has the ith genotype. A genotype's evolutionary activity (or "activity," for short) reflects the changes in its adaptedness (relative to the other genotypes in the population) throughout its history in the system.

Concentration might be an inappropriate measure of a genotype's adaptive significance in some contexts; In this case, the definition of evolutionary activity would need to operationalize adaptive significance in some other way. Furthermore, when concentration is impractical to measure, the definition of evolutionary activity must be appropriately modified. For example, since concentration data are generally unavailable for taxonomic families in the fossil record, evolutionary activity for fossil families could be defined by integrating a family's *presence* in the fossil record [12]. The key in each case is to increment a genotype's activity counter a_i over time by some method that reflects the genotype's relative adaptive significance. Then the integration in Equation 1 makes the activity counter a_i reflect the history of the genotype's adaptive significance.

To summarize the evolutionary activity of all the genotypes throughout the history of evolution in a system, we define an *activity distribution function*, $M(t, a)$, as follows:

$$M(t, a) = \begin{cases} 1 & \text{if there exists } i \text{ such that } a_i(t) = a \\ 0 & \text{otherwise.} \end{cases} \tag{2}$$

The activity distribution function combines information about how the activity $a_i(t)$ of every genotype i in the population changes over time.[1] Our visualization method is simply to graph these activity distribution functions.

Evolutionarily significant genotypes trace a salient line or "wave" in activity distribution graphs. Comparing evolutionary activity waves within or between systems can show how these evolutionary phenomena vary as a function of time, space, mutation rate, mode of selection, or other factors. In addition, the data displayed in this visualization method can be quantified with various statistics [7, 11–13], thus enabling

1 This $M(t, a)$ distribution function omits some of the information reflected in the original definition [11]. The strict analogue of the original definition would reflect the *number* of genotypes that have a given activity value at a given time, as follows:

$$N(t, a) = \#\{i\colon a_i(t) = a\}, \tag{3}$$

where $\#\{\cdot\}$ denotes set cardinality. For present purposes the simpler definition in the text suffices.

evolutionary activity in various artificial and natural systems to be directly compared [12, 13]. And because one can argue that the nature of life is intrinsically connected with adaptive evolutionary activity [8, 9], this visualization method can put discussions of the nature of life on a vivid, empirical footing.

In the rest of this article, after describing the evolutionary model used here, we explain how to interpret activity distribution functions, examine the adaptive phenomena evident in the activity distribution functions from a handful of individual runs of the model, and finally indicate the generality of this method. Although we illustrate the visualization method in the Evita model here, the method applies directly to any other system with an evolving distribution of genotypes. Comparing our detailed visualization of evolutionary activity of genotypes with the original application of this method to individual alleles [11] should help to convey how easily this method can be adapted to display and quantify evolutionary activity at a variety of different levels in a variety of different kinds of evolving systems.

2 The Evita Model and a Nonadaptive Analogue

The Evita model consists of a population of self-replicating strings of code competing for space, akin to Tierra [30] and Avida [3]. As in Tierra and Avida, programs in a customized assembly language carry out their own replication while subject to mutation. Unlike Tierra but like Avida, these programs interact only with their nearest neighbors on a two-dimensional grid, so the spread of information through the population depends on the size of the system. But Evita is much simpler than Tierra and Avida because it disallows code parasitism and thus blocks parasitism and more complicated interactions (e.g., hyperparasitism and code pirating), so Evita's dynamics are especially easy to understand. We use such a simple system here to provide an especially simple and clear illustration of our visualization method. In addition, understanding Evita should help illuminate more complicated analogues such as Tierra and Avida. Indeed, the visualization method we introduce here would be an especially useful tool to use for studying these more complicated systems.

Evita is initialized with a single human-written program placed randomly on an $N \times M$ grid. This program then executes and thereby reproduces. Each offspring is placed within a small radius of the parent program on the grid, and they then also start executing. When a parent program can find no unoccupied grid locations nearby, the system chooses randomly from the oldest of its neighbors, "kills" that neighbor, and places the offspring there. No other interaction between programs is permitted.

A time step of the model is a unit of time in which the program at each occupied grid spot receives a fixed amount of the processor time. This time is allocated in a way that is unbiased by position; hence, no organism can gain an advantage in its placement. In fact, the only real advantage position can give is the relative fitness of the surrounding population: It may be that the nearby creatures are less fit, for example, reproduce more slowly, than the creature placed onto their edge.

Mutations in this model are all point mutations, and they can fall on any existing program at any time, as if caused by "cosmic-rays." The mutation rate is specified in terms of the probability per time step that each given "codon" or assembly language instruction in a genotype is mutated to another instruction (chosen at random with equal probability from the entire instruction set). Thus, the probability that a given program suffers a mutation somewhere is proportional to its length. While the probability that a given program is mutated is independent of the size of the population of programs, the probability that a mutation occurs somewhere in the population is clearly proportional to the population size. Typically, mutation rates are specified in terms of 10^{-5} mutations per time step: That is, a mutation rate of m would mean that a given codon would

mutate on average once every $10^5/m$ time steps. This means, for example, that in a run with 1,600 creatures with an average length of 30 instructions, a mutation rate of 1 would cause one mutation somewhere in the population approximately every other time step. By increasing the mutation rate to 200, the population generally dies out almost immediately because no successfully reproducing creature can survive long enough.

The model has a clear biological analogy. The system represents a biological "soup," full of self-replicating strands of code (similar to RNA). Survival is governed primarily by reproductive speed, and evolution toward faster programs is the behavior usually exhibited. This kind of system, while extremely simple, shows interesting behavior in certain regimes of mutation rate. Many people have used Tierra, Avida, and similar systems to examine a variety of issues in evolutionary dynamics [1–4, 16, 17, 25, 30–35, 37].

There is a clear distinction between genotype and phenotype in Evita. A given genotype is defined simply as a string of assembly language code. If two programs differ in even one instruction they have different genotypes. On the other hand, two programs might have exactly the same behavior—the same phenotype—even though they have different genotypes. The fundamental reason for this is that the only behavior of these programs, the only thing they "do," is reproduce, so the only difference between the behavior of programs is the speed with which they reproduce. Thus, any two genotypes that reproduce at the same rate, no matter how different their genotype, will have exactly the same phenotype.

The distinction between genotype and phenotype becomes important whenever there is a piece of unused or unimportant code in the programs. For example, programs sometimes include instructions that are never executed. This code can then be mutated freely without affecting the operation of the program; multiple genotypes—without phenotype distinction and so with exactly the same fitness—may then arise and appear as different waves in the activity distribution pictures.

Evita is explicitly designed so that the only way the programs interact is by competing for space. On average, programs that reproduce faster will supplant their more slowly reproducing neighbors. A program's rate of reproduction depends only on its genotype. Here, we measure the rate at which a genotype reproduces, or its "fecundity," as we will call it, as the reciprocal of the number of instructions that must be executed for an instance of that genotype to reproduce, on average.[2] So, a genotype that uses half as many instructions to reproduce as a second genotype will have twice the fecundity of the second. A genotype's fecundity is the sole determinant of the expected rate at which programs with that genotype will produce offspring. Most significant adaptive events in Evita are changes in fecundity, so for present purposes we simply equate a genotype's fitness with its fecundity.[3] To keep fitness values from being inconveniently small, we define fitness as 30 times fecundity. So, for example, a genotype that reproduces in 100 instructions has a fecundity of 0.01 and a fitness of 0.3.

Two types of genetic changes can affect a genotype's fitness: change in length and change in algorithm. A change in length usually leads to a change in fecundity, that is, the time in which a program produces one copy (on average). Because adaptation is driven mainly by fecundity, shorter programs have a higher fitness, everything else being equal. In fact, a program typically gains a four-time-step decrease in reproduction

2 In biology, fecundity is the number of offspring that an individual produces. Note that our use of the term, though related, is different.

3 Shorter programs are more resistant to mutations (recall above), so a program's length influences its copy fidelity and, thus, its representation in future generations. Thus, fecundity is not a perfect measure of evolutionary success. Nevertheless, at the mutation rates used here, evolutionary success overwhelmingly reflects fecundity, so our definition of fitness is more than adequate for present purposes.

time for each codon that is "lost" from its length. But things are not always equal when an algorithm changes. To see why, consider a typical copy loop:

```
nop0    # marker, the complement of the marker nop2
dec     # decrement the (BX) register
copy    # copy an instruction
ifnz    # if register (BX) not zero,
jmp-b   # jump back to the complement of the next marker
nop2    # marker
...     # continued thread of execution
```

An archetypal copy-loop algorithm change is "unrolling the loop." Well known to assembly language programmers, it involves reducing the time spent in a loop by reducing the loop overhead. That is, by doing more within the actual loop code, one can reduce the number of times the loop is iterated, thus reducing the overall amount of flow control instructions executed in the loop. Here is a code example:

```
nop0    # an example of unrolling the loop
dec
copy
dec     # this second copy procedure
copy    # is contained in the loop
ifnz
jmp-b
nop2
```

This can lead to a significant increase in the speed of execution. Comparing the two examples, above, in the first loop one copy is performed every four instructions, while in the second loop two copies are performed in the space of six instructions, resulting in a 50% increase in speed even though the second algorithm uses 30% more code.

We also define a nonadaptive analogue of Evita, which differs from Evita only in that there is no chance that a genotype's presence or concentration in the population is due to its adaptive significance. Nominal "programs" exist at grid locations, reproduce, and die. The nonadaptive or "neutral" model has two parameters: the number of mutations in the population per time step and the number of "programs" that reproduce per time step; each of these parameters can be either a single average value or a varying sequence of particular values. When the neutral system is due to have a reproduction event, the self-reproducing "program" is chosen at random from the population (with equal probability). When a "program" reproduces, its oldest neighboring "program" dies and the new child occupies the newly emptied grid location. Each "program" has a nominal "genotype" that its children inherit. Whenever a mutation strikes a "program" it is assigned a new "genotype." The evolutionary dynamics in this neutral analogue is reduced to a simple positive random walk in genotype space [4]. Genotypes arise and go extinct, and their concentrations change over time, but the genotype dynamics is only weakly linked to adaptation through the reproduction rate parameter determined by the normal model. None of the dynamic of a genotype in the neutral analogue is due to that genotype's adaptive significance, for a genotype has no adaptive significance whatsoever.

By recording mutation rates and reproduction rates from an actual Evita run, the nonadaptive analogue can then be run with these parameters. The behavior of this neutral analogue allows us to determine which aspects of the behavior of our original

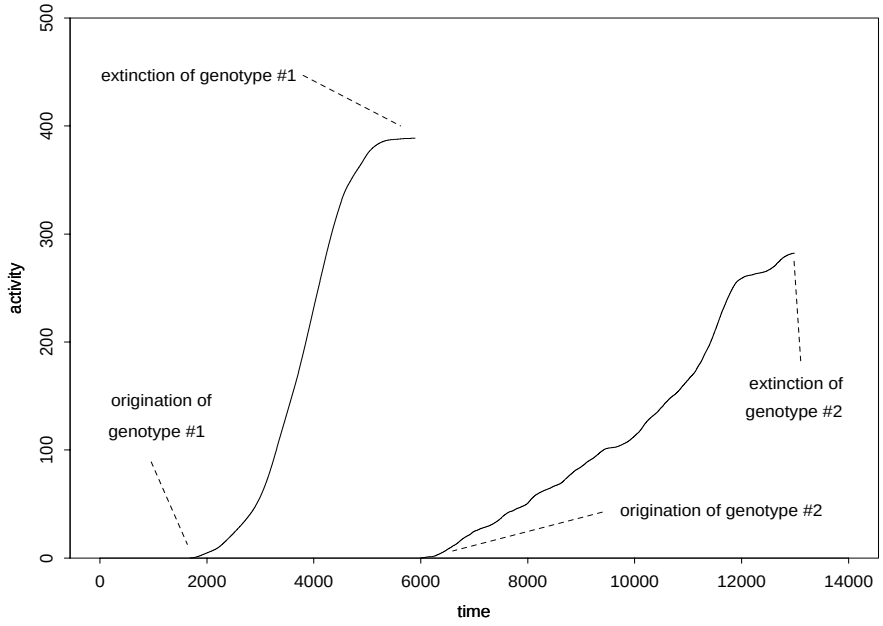

Figure 1. An illustration of two isolated genotype activity waves, taken from two activity distribution functions. The origination and extinction of each genotype is clearly visible. A genotype's concentration at a given time is proportional to the slope of its activity wave at that time. Thus, the wave's slope increases (or decreases) when the genotype's concentration in the population rises (or falls), and the genotype becomes extinct when the wave's slope falls to zero. A point in the graph of an activity distribution function $M(t, a)$ represents a binary characteristic; $M(t, a)$ is either 0 or 1 at the point (t, a), depending on whether any genotype in the system has activity a at time t (recall Equation 2).

Evita run were due to adaptation and which can be attributed to nonadaptive factors such as chance (e.g., random genetic drift) or necessity (e.g., the system's underlying architecture). A series of related studies has similarly exploited nonadaptive or "neutral" models [7, 12, 13].

3 Interpreting Activity Wave Diagrams

Graphs of activity distribution functions depict how evolutionary activity of the genotypes (on the y axis) varies as a function of time (on the x axis). The most evident feature of such graphs is the presence of myriad lines or *waves* (as we will call them), clearly evident in the figures below. Each wave corresponds to a single genotype and shows the variation over time of that genotype's evolutionary activity.

It follows directly from the definition of evolutionary activity that the slope of a given genotype's activity wave at a given time is the same as the genotype's concentration in the population at that time. This explains why the waves invariably arise from the x axis and thence move upward and rightward, as illustrated by the two isolated waves in Figure 1. When a new genotype enters the population, a new wave will arise from the x axis. As the genotype's concentration in the population grows (or shrinks) over time, the slope of the wave increases (or decreases). When the genotype finally goes extinct, the slope of its wave falls to zero and the wave ends. In this way, a genotype's activity wave reflects its changing concentration throughout its history in the population.

Thus, an activity distribution function graph depicts the adaptive history of every genotype in the population. The ancestral genotype always corresponds to the wave that arises out of the origin. (See any of the activity distributions below.) When the ancestral genotype is driven to extinction by another genotype, the ancestral wave ends as one or more new significant waves arise. Whenever one genotype drives another to extinction, a new wave arises as an earlier one dies out. Multiple waves coexist in the activity diagram when multiple genotypes coexist in the population, and genotypic interactions that affect genotype concentrations are visible as changes in the slopes of waves. In general, the dominating genotype(s) during a given epoch of evolution appear as dominating wave(s) during that period of the activity diagram.

Mutation rate has a direct and obvious impact on the evolutionary dynamics of genotypes, and this effect is clearly evident in the genotype's activity wave diagrams. Comparing the activity waves in a series of runs in which all parameters are held constant except for mutation rate shows how evolutionary activity phenomenology depends on mutation rate (Figure 2). When the mutation rate is set to zero, there is just one genotype—the ancestral one—so there is just one wave with constant maximal slope (slope $= 1$). As soon as the mutation rate becomes positive, new waves start to appear throughout the course of the runs, and their changing concentration in the population causes the waves' slopes to vary. The rate at which new waves are generated is proportional to the mutation rate, and the length of waves is inversely proportional to the mutation rate, just as one would expect. (The choice of scale for x or y axes on a graph of an activity density function can obscure the density or length of activity waves, so these proportionalities are not always evident.)

When we compare activity wave diagrams from the normal Evita model and its neutral analogue, we see a dramatic indication of how activity distribution functions highlight significant adaptive events. To produce a neutral analogue that is directly comparable with a normal Evita run, we recorded the reproduction rate per time step and the mutation rate per program per time step from the normal Evita run and then ran the neutral model with these sequences of values as input. Figure 3 compares the activity distribution functions from these normal (top) and neutral (bottom) runs, with the activity scale (y axis) in these two plots set to be roughly comparable.

There is a striking difference between these two graphs; leaving aside the ancestral wave, the highest waves in the normal Evita model are three orders of magnitude higher than those in the neutral analogue.[4] This is clear evidence of how the size of a genotype's activity waves in the normal Evita data reflects the genotype's adaptive significance. In the normal model, at each time one or a few genotypes enjoy a special adaptive advantage over their peers, and this is reflected by their correspondingly huge waves. In the neutral analogue, by contrast, a genotype's concentration reflects only dumb luck, so no genotype activity waves rise significantly above their peers. This difference between the normal and neutral activity data can be used to quantify the adaptive evolutionary activity in evolving systems [7, 11, 13].

4 Details in Individual Activity Wave Diagrams

In this section we discuss the specific evolutionary phenomena visible in a handful of Evita runs driven by different mutation rates and lasting for different durations. This detailed analysis of a variety of individual runs is the best way to convey how activity wave diagrams can depict a variety of evolutionary phenomena, such as competitive exclusion and random genetic drift. To help interpret the adaptive significance of

4 The other salient difference between the normal and neutral runs—that the ancestral genotype persists about four times longer in the neutral run—is due to the fact that, since the neutral ancestral genotype need never compete with better adapted genotypes, its initial numerical advantage as ancestor carries more weight.

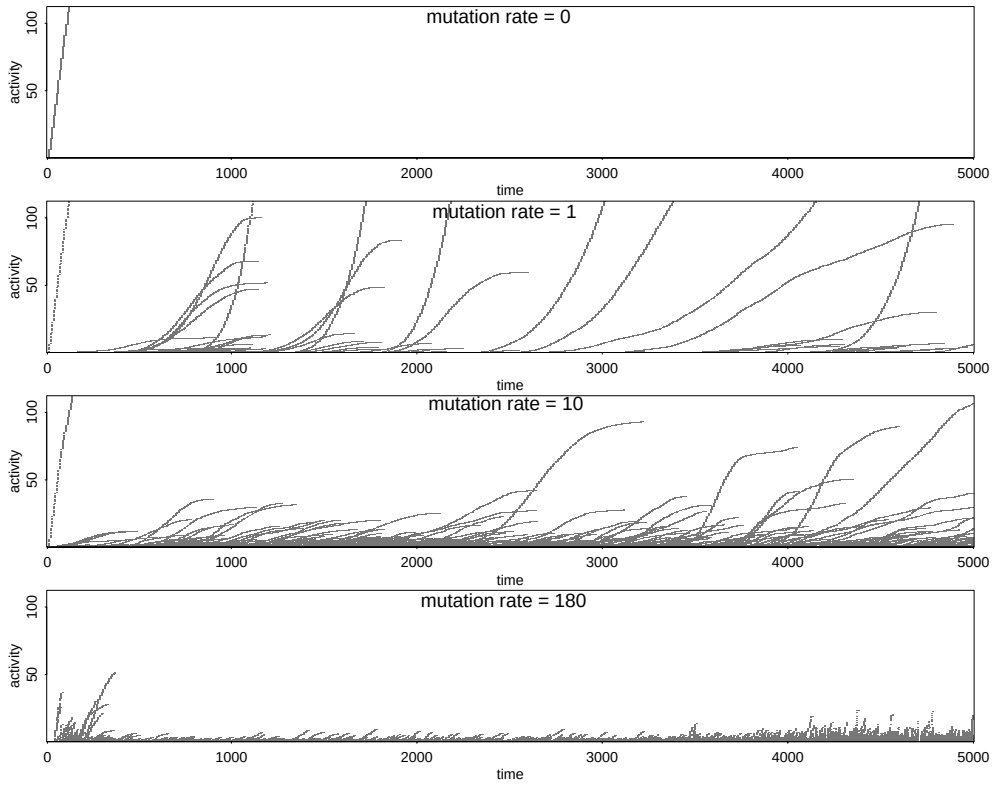

Figure 2. Activity distribution functions, $M(t, a)$, showing genotype activity waves at different mutation rates. Note that the time and activity scales on all graphs are the same, so the activity wave phenomenology is directly comparable. The activity scale causes some activity waves to be cropped. The activity distribution function at mutation rate $= 0$ shows only one wave (cropped very early in the run) because the system can contain only one genotype—the ancestral genotype. This wave is a straight line with slope one persisting for the duration of the run. In general the number of waves (new genotypes) is proportional to the mutation rate and the length of waves (duration of genotypes) is inversely proportional to the mutation rate.

the activity waves, we compare the activity diagrams with fitness plots of the same runs and we confirm our interpretations by examining the specific assembly language instructions in the relevant genotypes.

In all the runs shown below we held constant all model parameters except mutation rate and elapsed time. The grid size was 40×40, so when the grid filled up the population consisted of about 1,600 self-reproducing programs. To prune out irrelevant data about transitory genotypes all the activity distribution functions shown here depict only those genotypes that at one time have more than a certain minimum representation (five copies) in the population.

Each genotype in a given run is given a unique name of the form *AB*, where *A* is a number indicating the genotype's length and *B* is a three-character string (in effect, a base 52 number) indicating the genotype's order of origination among genotypes of that length. Thus, `32aac` is the third length-32 genotype to arise in the course of a given run.

4.1 Mutation Rate = 1; 5,000 Time Steps

The activity graph (Figure 4) of this run is dominated by five waves corresponding to the five most populous genotypes over the course of the run. Miscellaneous low-

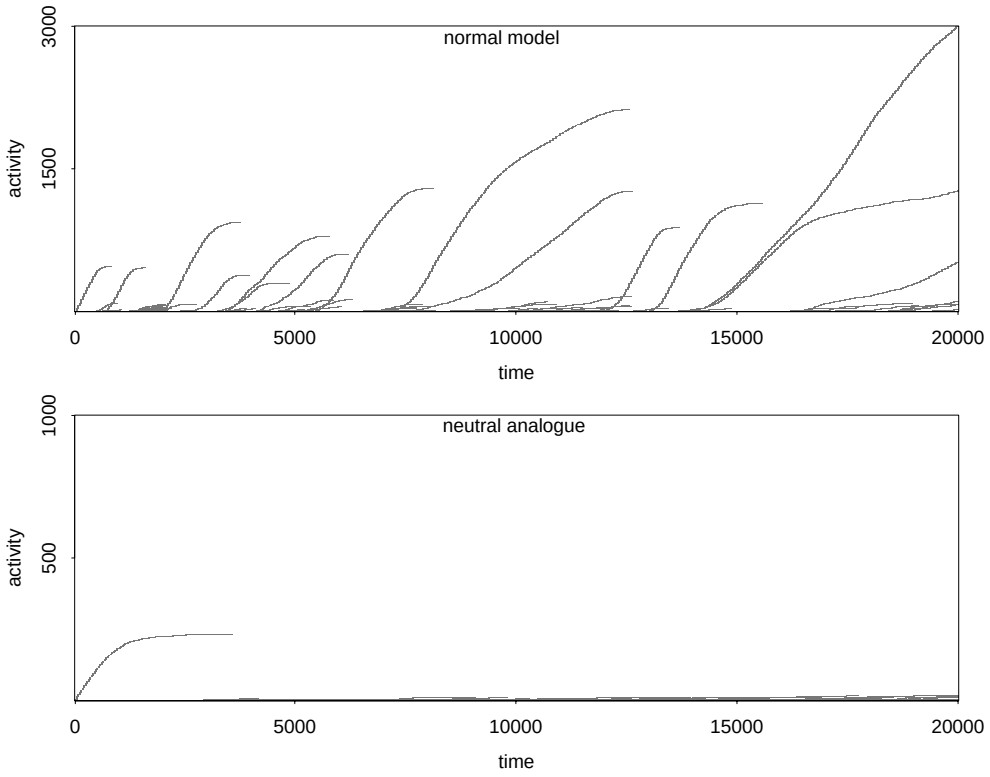

Figure 3. Genotype activity waves in activity distributions $M(t, a)$ from a normal Evita run (top) and from a run of the neutral analogue (bottom). The parameters used to drive the neutral analogue were taken directly from the normal run. Note that the activity scale on the normal model data is three times that of the neutral analogue; comparable activity scales would make the waves in the normal model three times higher than those shown here.

activity genotypes that never claim a substantial following in the population are barely visible along the bottom of the activity plot.

Comparison with the fitness plot shows that each of the significant new waves corresponds to a genotype that has a significant fitness advantage over its predecessors, and closer examination of those genotypes discloses those adaptive advantages. The first significant new wave is caused by genotype `33aad`, which reproduces much faster than the ancestral genotype `37aaa` due to its shorter length. The next significant activity wave, the largest one in the graph, is caused by genotype `33aak`; this genotype is the same length as `33aad` but it can reproduce faster because it has a shorter copy loop. Notice the kink in `33aak`'s wave at about time step 2000. Magnifying the low-activity waves at that time shows that this kink is simultaneous with the start of another wave—the fourth main wave in this plot, due to genotype `31aab`, which is still shorter in length. The post-kink slope in `33aak`'s wave is slightly less than that of `31aab`'s wave, and in fact genotype `31aab`'s shorter length gives it only a slight fitness advantage (about 1%) over genotype `33aak`. Finally, the fifth significant wave is caused by a genotype, `30aab`, which reproduces faster than genotype `31aab` due to its slightly shorter length.

Thus, we see that the activity distribution plot clearly highlights those genotypes with a significant adaptive advantage over their peers. In addition to births and deaths of genotypes, we clearly see the dynamics of competitive exclusion between the major genotypes in the evolving system.

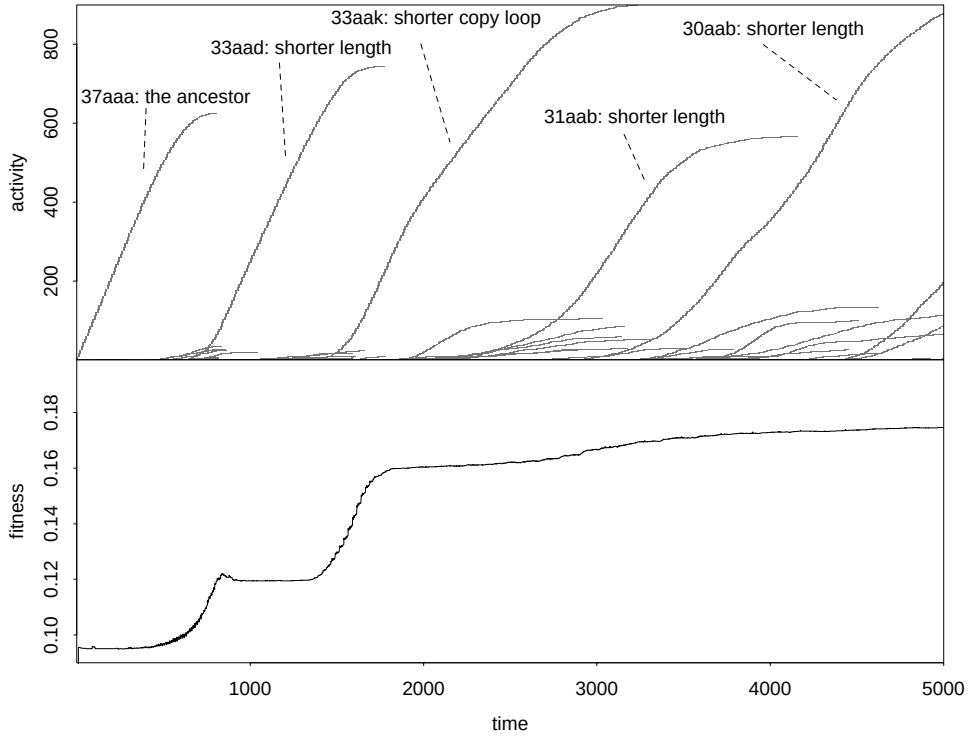

Figure 4. Genotype activity distribution function $M(t, u)$ from a typical run with mutation rate = 1. Above: graph of $M(t, a)$ showing genotype activity waves. Below: average genotype fitness. The genotype causing each salient wave is indicated, and its adaptive advantage over its predecessors is noted. Note that the start of a significant new wave corresponds to an increase in fitness.

4.2 Mutation Rate = 2; 5,000 and 20,000 Time Steps

The data from this run (Figure 5) shows a nice correspondence between the main activity waves in the activity distribution plots and the main fitness jumps, as in the previous run. Closer analysis reveals the same general pattern as before: The major activity waves correspond to the major adaptive events, and these consist of shortening a genotype's length or copy loop. But there are two interesting exceptions to this general pattern. Each exception involves a distinctive kind of evolutionary phenomenon, and each leaves a characteristic signature in activity wave diagrams.

One exception is that the second fitness jump corresponds to a cluster of seven similar genotypes (`33aap, 33aaq, 33aar, 33aas, 33aat, 33aau, 33aav`) that all arise at about the same time and together contribute to a dense cloud of activity waves; see Figure 6. These genotypes differ from each other only by mutations at an unexpressed locus, so they all use exactly the same algorithm and are neutral variants of one another—different genotypes with exactly the same phenotype. The unexpressed locus was created by a mutation that produced a nontemplate instruction inside the template surrounding the copy loop, saving one executed instruction per loop traversal and thus significantly increasing fecundity. Once this mutation has occurred, almost any other mutation at the same locus creates another nontemplate instruction with an identical fitness benefit, so a cloud of neutral variants quickly grows. Because these neutral variants have exactly the same fitness advantage over their predecessors, and

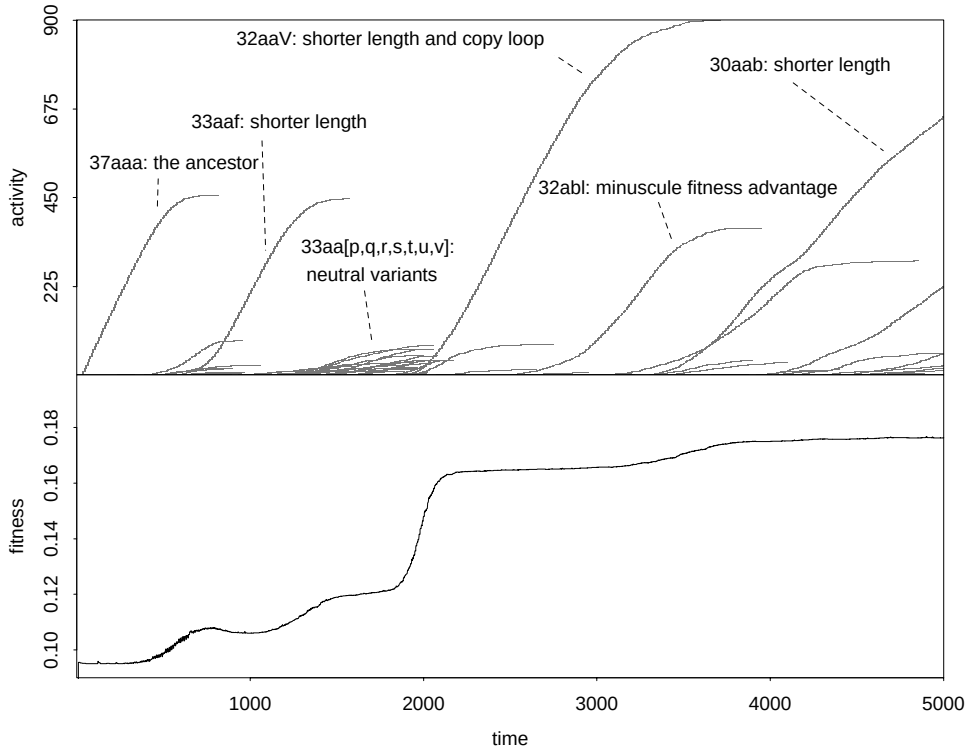

Figure 5. Genotype activity distribution function $M(t, u)$ from a typical run with mutation rate $= 2$, 5,000 time steps. Above: graph of $M(t, a)$ showing genotype activity waves. Below: average genotype fitness. The adaptive advantage of the genotypes causing the salient waves is indicated. The start of a significant wave generally corresponds to an increase in fitness. Note the cloud of neutral variants that cause one of the fitness jumps and act in the population like a single phenotype. These neutral variants are more fit than `33aaf` because they require one fewer instruction per execution of the copy loop. Note also that the significant wave due to genotype `32abl` does *not* cause a significant fitness increase. Genotypes `32abl` and `32aaV` are nearly neutral variants that coexist without significant adaptive competition, for `32abl` executes only one fewer instruction per reproduction event than `32aaV`.

because they all are just one mutation away from each other, they engage in adaptive interactions with competing genotypes effectively as a single higher-level unit. If the activity data from these neutral variant genotypes were pooled and graphed as a single phenotype, they would constitute a single salient wave on a par with the other salient waves in the activity distribution function.

Second, notice that the fourth salient wave (due to genotype `32abl`) does *not* correspond to a significant fitness jump. The fact that the waves from `32aaV` and `32abl` coexist for a long time (about 1,000 time steps), rather than one quickly driving the other to extinction by competitive exclusion, indicates that they are nearly neutral variants. In fact, the fitness of the second wave (`32abl`) exceeds that of the first wave (`32aaV`) by about only 0.5%, for `32abl` has a mutation that causes a single instruction to be skipped, for a net savings of one instruction per reproduction event. The interactions among the three salient waves between time steps 4000 and 5000 have a similar explanation. They are a significant improvement (5% fitness advantage) over the genotypes that they drive extinct, but they differ from one another by much less (under 2% fitness difference).

When this run is extended significantly further (Figure 7), we continue to see compet-

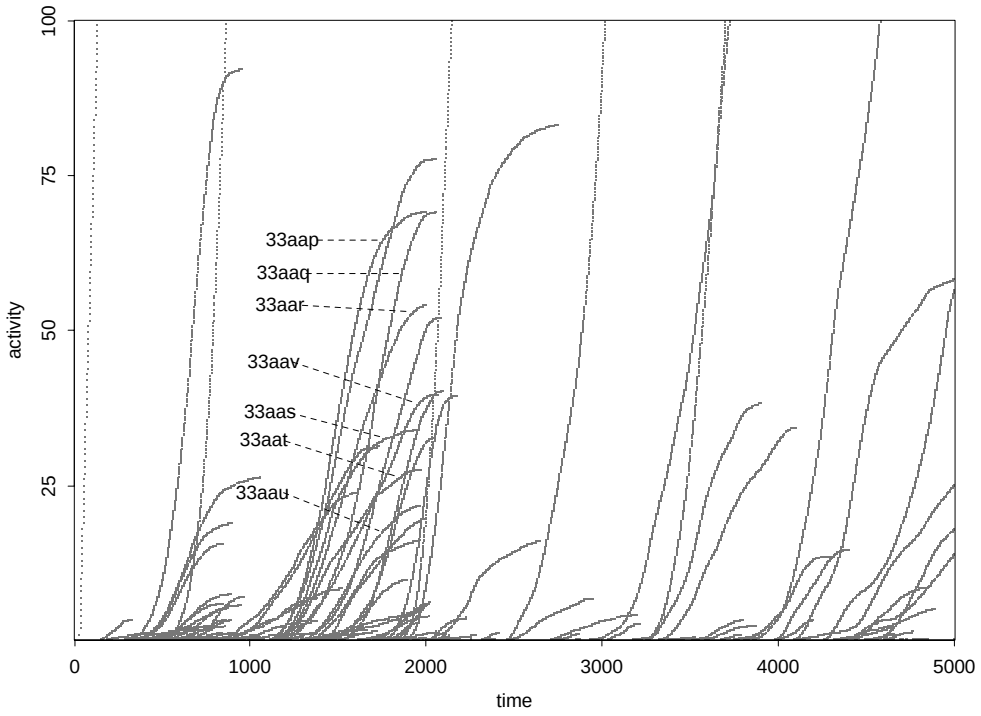

Figure 6. Blow up of the activity distribution function $M(t, u)$ from the run with mutation rate $= 2$, 5,000 time steps, magnifying low activity. The neutral variants shown here cause the fitness increase that occurs just after time step 1000 (see Figure 5).

itive exclusion between genotypes when the origination of one genotype wave causes the end of another, and we also continue to see neutral variants when significant genotype waves persist simultaneously for a significant duration.

4.3 Mutation Rate = 10; 20,000 Time Steps

This run (Figure 8) shows some classic competitive exclusion during the first 2,000 time steps, in which significant fitness boosts correspond to the origination of significant new genotype waves. But evolution reaches an equilibrium early in the run and the bulk of the evolutionary change in the run consists of random drift among selectively neutral genotypes—the sort of neutral evolution emphasized by Motoo Kimura [23]. The difference between these kinds of evolutionary phenomena is clearly indicated in the different quality of the activity waves. A genotype winning at competitive exclusion typically causes a relatively smooth and sigmoidal-shaped wave (although the bottom of the wave will be truncated if its concentration rises extremely fast). By contrast, random drift causes waves that are much more wiggly because the wave's slope randomly rises and falls as the genotype's concentration wanders up and down. This difference can be clearly seen in Figure 1. The sigmoidal wave in Figure 1 is that due to genotype `32abl` in Figure 5, which arose through competitive exclusion, and the wiggly wave in Figure 1 is taken from the random genetic drift in the middle of Figure 8.

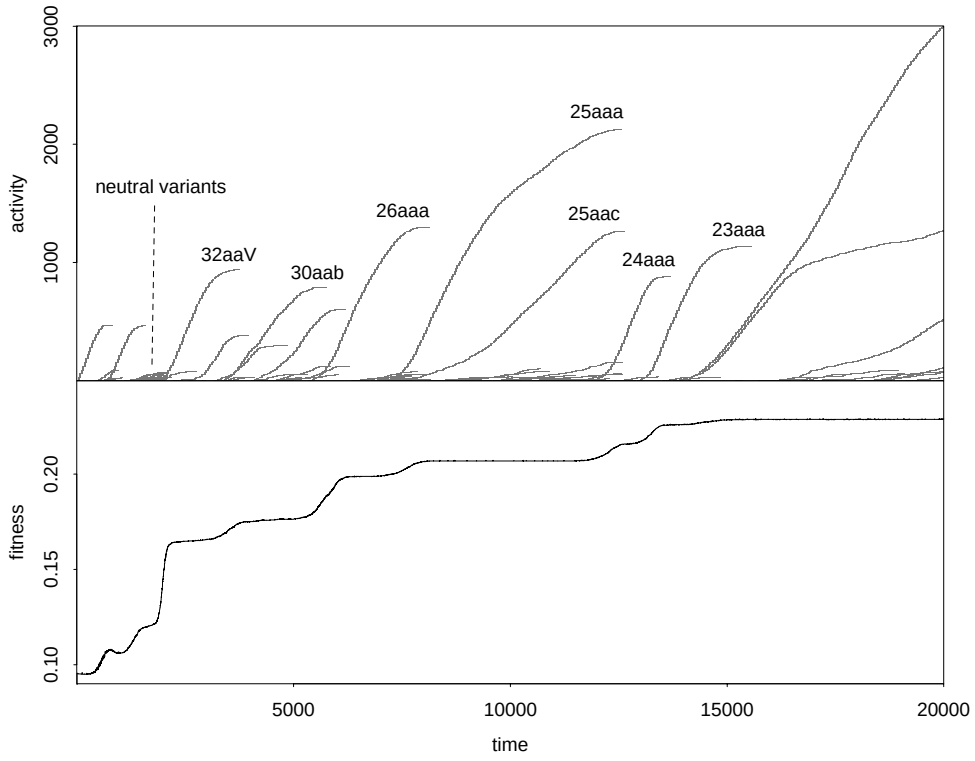

Figure 7. Genotype activity distribution function $M(t, u)$ from a typical run with mutation rate = 2, 20,000 time steps; this is a continuation of the run shown in Figure 5. Above: plot of $M(t, a)$ showing genotype activity waves. Below: average genotype fitness. Genotypes corresponding to some of the salient waves are marked. Note that the evident adaptive advantage of the salient waves is being shorter in length than their competition. The significant coexistence of waves is a sign of selectively neutral variants. For example, the two simultaneous waves in the middle of the run are due to the neutral variant genotypes `25aaa` and `25aac`. Other neutral variants are also evident during this run. With the exception of the origination of neutral variants, the start of each significant wave corresponds to an increase in fitness.

4.4 Mutation Rate = 40; 30,000 Time Steps

This run (Figure 9) shows a variety of evolutionary phenomena. First, standard competitive exclusion between genotypes dominates the first 3,000 time steps of the run; some of this is evident in the familiar sigmoidal wave shapes, but some is hidden in low-lying clouds of neutral variants acting as a single phenotype. Next, as the rather wiggly waves signal, over half of the run consists of random genetic drift among more or less neutral variants with minute differences in fitness. It is interesting to note that genotype `24aNR`, which creates the last and longest wiggly wave in the middle of the run, takes two *more* instructions to reproduce, and so is slightly *less* fit, than the genotype (`24avp`) that it supplants. This illustrates how marginal fitness improvements do not always win the day during random drift.

At about two-thirds the way through the run we see the emergence of a new genotype (`24bxI`) that totally dominates the rest of the run. Genotype `24bxI` has a huge fitness advantage (about 20%) over its competitors because it has acquired the ability to "unroll the loop." (Shortly before this the genotype `24bqf` acquired a slight fitness advantage by partially unrolling the loop.) The run ends in a period of evolutionary equilibrium, with a variety of new genotypes coexisting with the original loop unroller

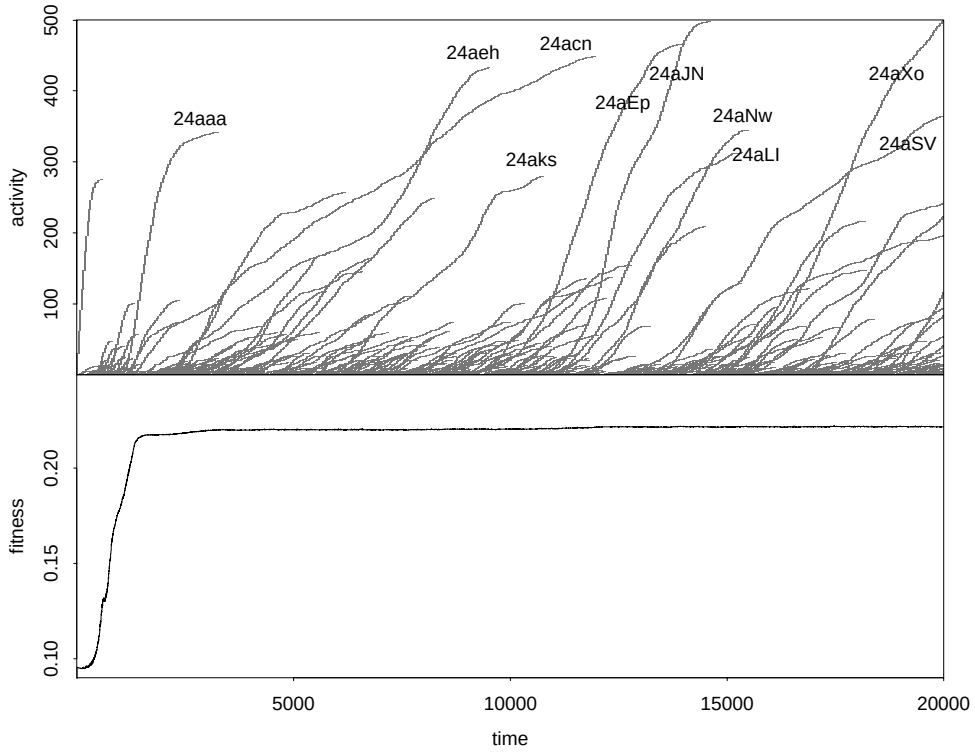

Figure 8. Genotype activity distribution function $M(t, u)$ from a typical run with mutation rate = 10. Above: plot of $M(t, a)$ showing genotype activity waves. Below: average genotype fitness. Evolution reaches an equilibrium early in this run. The last genotype clearly arising through competitive exclusion is `24aaa`. The rest of the evolution seen here is dominated by random genetic drift among selectively neutral genotypes. Some of the neutral variants of `24aaa` undergoing random genetic drift are indicated. Note the quite different quality of the sigmoidal activity waves due to competitive exclusion and the wiggly waves due to random genetic drift. The wiggly wave from genotype `24aks` was shown out of context in Figure 1.

and undergoing random genetic drift. These new genotypes are all neutral variants of the original loop-unrolling genotype, differing only by unexpressed mutations.

4.5 Mutation Rate = 30; 178,000 Time Steps

This run (Figure 10) is an order of magnitude longer than any other shown here. We see that significant adaptations can continue to happen in the Evita model after quite long periods of stasis. The fitness jump at about time step 10000 occurred when a genotype (of length 24) first acquired the ability to unroll the loop. The two subsequent significant fitness jumps correspond to shorter loop-unrolling programs, of length 22 and 20, respectively. The long periods between these adaptive innovations consist of random drift among neutral variants of these loop unrollers.

Of particular interest is the period (roughly spanning time steps 40000–80000) that has *no* salient waves at all—a unique occurrence in the runs shown here. This period starts with the innovation of a length-22 loop-unrolling genotype, but this genotype is quickly supplanted by a sequence of selectively neutral variants, each of which quickly supplants its selectively neutral predecessor. All of these neutral variant genotypes differ only in silent mutations at two unexpressed sites, and so all have exactly the

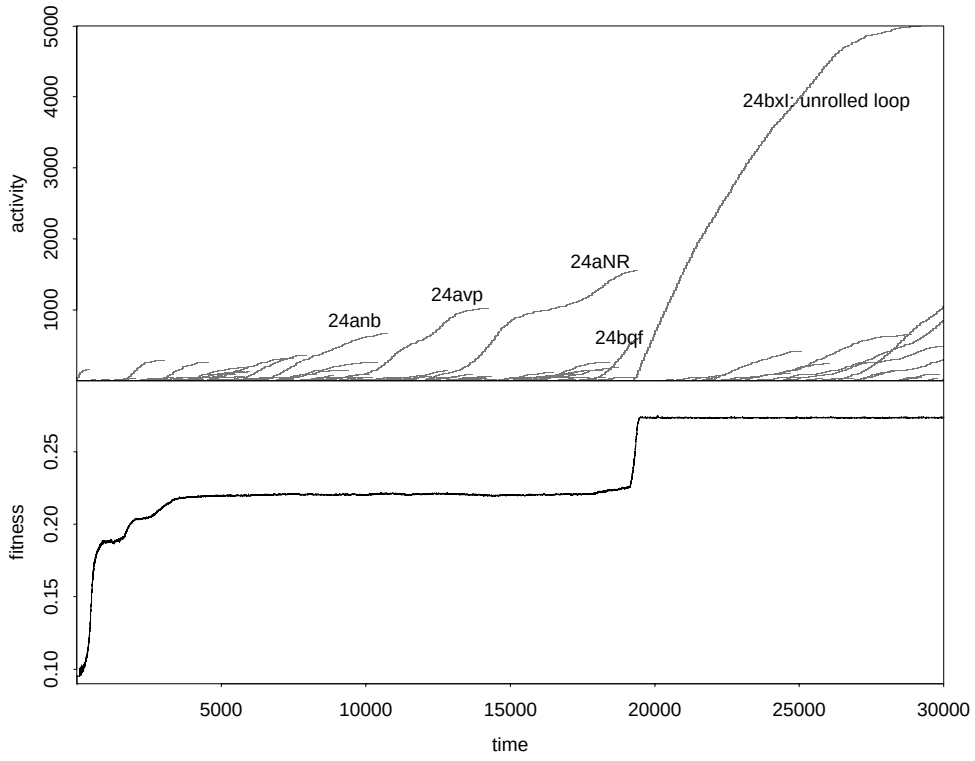

Figure 9. Genotype activity distribution function $M(t, u)$ from a typical run with mutation rate = 40. Above: plot of $M(t, a)$ showing genotype activity waves. Below: average genotype fitness. Competitive exclusion is evident in the first 3,000 time steps of the run and at time step 20000 when genotype `24bxI` discovers the loop unrolling algorithm. Most of the other salient genotype activity wave phenomena is random drift of nearly neutral variants; note the substantial periods of flat fitness. The quality of the activity waves signals the difference between adaptively significant evolution (sigmoidal waves) and the genetic change during periods of adaptive stasis (the wiggly waves of neutral variants). Nearly neutral variants are not always exactly neutral. For example, the three significant waves in the middle of the run (prior to the discovery of unrolling the loop) are due to genotypes `24anb`, `24avp`, and `24aNR`, which have fitnesses of 0.222, 0.224, and 0.220, respectively. These fitnesses, though close, are not identical. Nevertheless, note that genotype `24aNR` is still able to supplant genotype `24avp` even though its fitness is slightly lower (0.220 vs. 0.224). Random genetic drift among nearly neutral variants can swamp slight fitness advantages.

same fitness. Magnifying the waves corresponding to these neutral variants would reveal the wiggly signature of random genetic drift.

The striking lack of salient waves during time steps 40000–80000 implies that the random drift during this period involves an unusually high density of neutral variant genotypes. The explanation for this high density is due to the *two* loci undergoing random drift in these genotypes. Two drifting loci create an order of magnitude more possible neutral variants than one drifting locus, and mutations produce these neutral variants at twice the rate.

5 Generalizations and Conclusions

Activity wave diagrams vividly show the evolving adaptive history of genotypes in the Evita model. Comparing activity waves from the normal Evita model with fitness graphs and with activity waves in a nonadaptive analogue shows how the significant activity waves have readily interpretable adaptive significance. Activity distribution diagrams

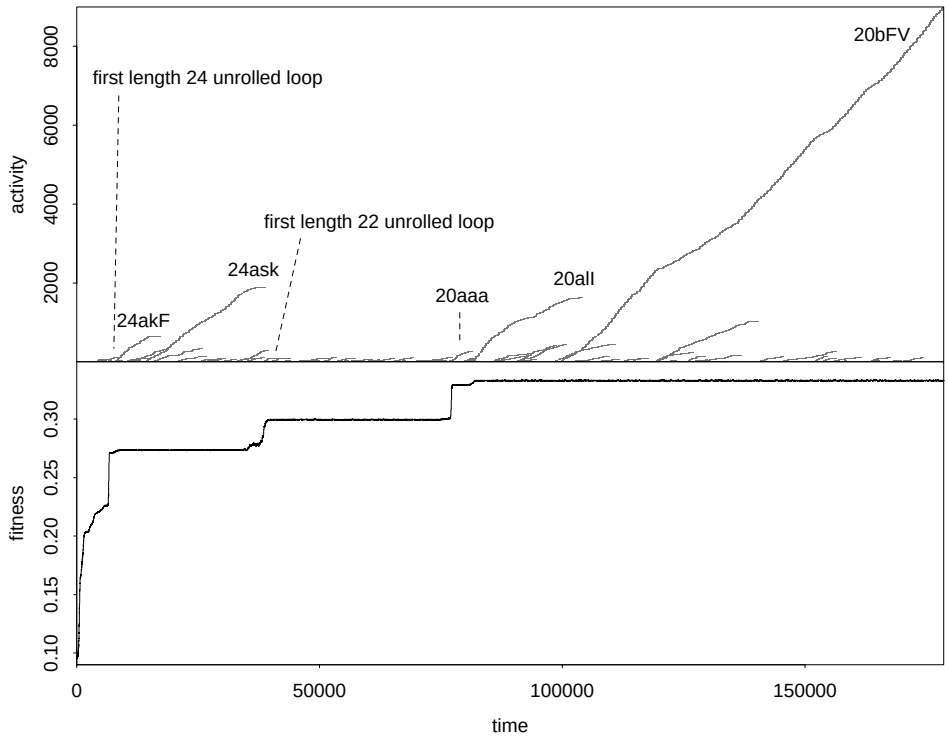

Figure 10. Genotype activity distribution function $M(t, u)$ from a typical run with mutation rate = 30. Above: plot of $M(t, a)$ showing genotype activity waves. Below: average genotype fitness. Three genotypes with successively shorter loop-unrolling algorithms cause the three largest fitness jumps. Between these adaptive innovations there is random genetic drift among selectively neutral versions of these algorithms. The genotypes of the largest activity waves in these periods of random drift are indicated.

show the number, timing, and character of a variety of adaptive phenomena, including competitive exclusion between genotypes, collateral evolution of selectively neutral variants, and random genetic drift. Somewhat akin to the interpretation of tracks in a cloud chamber, one can identify and read the history of different kinds of adaptive events in the waves in an activity distribution function.

Any system with an evolving distribution of genotypes can generate activity distribution functions, and such distributions make it easy to compare adaptive phenomena across a variety of artificial and natural evolutionary systems. We have made preliminary studies of activity distribution functions for genotypes in many different systems, including Holland's Echo model [21, 22], Packard's Bugs model [11, 28], Lindgren's model of evolving strategies in the iterated prisoner's dilemma [24], Ray's Tierra model [30], the Avida model of Adami and Brown [3], Arthur's El Farol model [5], and the Santa Fe artificial stock market of Arthur, Holland, LeBaron, Palmer, and Taylor [6, 29]. We have also made analogous studies of activity distribution functions for taxonomic families in the fossil record [14, 36].

In general, activity distributions from other systems have the same kind of interpretation as those given here for the distributions from Evita, but there are certain obvious differences in some cases. Some details of the interpretation depend on the definition of evolutionary activity, so modifying the definition can change the interpretation. One

simple example of this arises in those contexts in which it is appropriate to define a genotype's evolutionary activity by integrating its persistence rather than its concentration [12, 13]; in this case the activity waves are all straight parallel lines with slope equal to one. Some other details of interpretation depend on the nature of the evolutionary process that generated the data. One important example of this is our interpretation of wiggly activity waves. In the Evita model wiggly waves indicate random drift among selectively neutral variants. In other models, though, wiggly waves—especially certain kinds of coordinated wiggling—can signal various other kinds of interactions (such as host/parasite and cooperative interactions) that Evita disallows. We have focused in this article on visualizing evolutionary phenomena in the relatively simple Evita model to make the interpretation of the activity distributions especially simple and clear.

Evolutionary activity can be defined at levels other than the genotype, so activity distribution functions can depict evolutionary phenomena at other levels. For example, evolutionary activity has been observed at the level of individual genes [11], classes of genes [10], and taxonomic families in the fossil record [12, 13]. Analogous distribution functions could also be defined at the level of the phenotype, for example, by putting genotypes with effectively the same phenotype into equivalence classes. Furthermore, collecting activity statistics for genetic schemata would reveal the different schemata's relative adaptive significance, and this would allow one to judge the relative timing and magnitude of the evolutionary activity of different size schemata, for example.

Activity distribution functions do not just provide a qualitative visualization of evolutionary activity; they also enable us to define various *quantitative* aspects of evolutionary activity, including both what we might intuitively call an evolving system's "accumulated adaptive activity" [7, 12, 13] and what we might intuitively call its "adaptive evolutionary innovation" [11, 13]. Quantitative comparison of adaptive evolutionary activity across many different evolutionary systems, both artificial and natural, would open the door to a general study of the essential features of complex adaptive systems.

No single method can unambiguously show all aspects of all kinds of adaptation in evolving systems; activity wave diagrams are no exception. Still, these diagrams do flexibly apply to virtually all evolutionary systems. They are remarkably effective for visualizing a system's adaptive evolutionary activity, and they provide the foundation for a general quantitative study of adaptive evolutionary dynamics.

Acknowledgments

Special thanks to Norman Packard—longtime collaborator on methods for visualizing and quantifying adaptive evolutionary activity. Thanks to the Santa Fe Institute for support and hospitality while some of this work was completed. For helpful discussion on these issues, thanks to the audience at the Santa Fe Institute where some of this work was presented in the summer of 1996. For helpful comments on the manuscript, thanks to Tim Taylor, to the anonymous reviewers for *ECAL97*, where this work was presented in the summer of 1997, and to the anonymous reviewers for this journal.

References

1. Adami, C. (1995). Learning and complexity in genetic auto-adaptive systems. *Physica D, 80,* 154–170.
2. Adami, C. (1995). Self-organized criticality in living systems. *Physics Letters A, 203,* 23–32.
3. Adami, C., & Brown, C. T. (1994). Evolutionary learning in the 2D artificial life system "Avida." In R. Brooks & P. Maes (Eds.), *Artificial Life IV* (pp. 377–381). Cambridge, MA: MIT Press/Bradford Books.
4. Adami, C., Brown, C. T., & Haggerty, M. R. (1995). Abundance-distributions in artificial life and stochastic models: "Age and area" revisited. In F. Morán, A. Moreno, J. J. Merelo, & P. Chacón (Eds.), *Advances in artificial life* (pp. 503–514). Berlin: Springer-Verlag.

5. Arthur, W. B. (1994). Inductive reasoning and bounded rationality. *American Economic Review, 84,* 406–411.

6. Arthur, W. B., Holland, J. H., LeBaron, B., Palmer, R., & Taylor, P. (1997). Asset pricing under endogenous expectations in an artificial stock market. In W. B. Arthur, D. Lane, & S. N. Durlauf (Eds.), *The economy as an evolving, complex system II* (pp. 15–44). Menlo Park, CA: Addison-Wesley.

7. Bedau, M. A. (1995). Three illustrations of artificial life's working hypothesis. In W. Banzhaf & F. Eeckman (Eds.), *Evolution and biocomputation—Computational models of evolution* (pp. 53–68). Berlin: Springer-Verlag.

8. Bedau, M. A. (1996). The nature of life. In M. Boden (Ed.), *The philosophy of artificial life* (pp. 332–357). New York: Oxford University Press.

9. Bedau, M. A. (1998). Four puzzles about life. *Artificial Life, 4,* 125–140.

10. Bedau, M. A., & Jones, T. (1994). Unpublished results produced at the Santa Fe Institute.

11. Bedau, M. A., & Packard, N. H. (1992). Measurement of evolutionary activity, teleology, and life. In C. G. Langton, C. Taylor, D. Farmer, & S. Rasmussen (Eds.), *Artificial Life II, Santa Fe Institute Studies in the Sciences of Complexity* (pp. 431–461). Redwood City, CA: Addison-Wesley.

12. Bedau, M. A., Snyder, E., Brown, C. T., & Packard, N. H. (1997). A comparison of evolutionary activity in artificial systems and in the biosphere. In P. Husbands & I. Harvey (Eds.), *Proceedings of the Fourth European Conference on Artificial Life* (pp. 125–134). Cambridge, MA: MIT Press/Bradford Books.

13. Bedau, M. A., Snyder, E., & Packard, N. H. (1998). A classification of long-term evolutionary dynamics. In C. Adami, R. K. Belew, H. Kitano, & C. Taylor (Eds.), *Artificial Life VI* (pp. 228–237). Cambridge, MA: MIT Press/Bradford Books.

14. Benton, M. J. (Ed.). (1993). *The fossil record 2*. London: Chapman and Hall.

15. Burian, R. M. (1992). Adaptation: Historical perspectives. In E. F. Keller & E. A. Lloyd (Eds.), *Keywords in evolutionary biology* (pp. 7–12). Cambridge, MA: Harvard University Press.

16. Cho, S.-B., & Ray, T. S. (1995). An evolutionary approach to program transformation and synthesis. *International Journal of Software Engineering and Knowledge Engineering, 5,* 179–192.

17. Chu, J., & Adami, C. (1997). Propagation of information in populations of self-replicating code. In C. G. Langton & T. Shimohara (Eds.), *Artificial Life V* (pp. 462–469). Cambridge, MA: MIT Press/Bradford Books.

18. Dawkins, R. (1989). *The selfish gene* (Rev. ed.). New York: Oxford University Press.

19. Dawkins, R. (1987). *The blind watchmaker: Why the evidence of evolution reveals a universe without design*. New York: Norton.

20. Gould, S. J., & Lewontin, R. C. (1979). The spandrals of San Marco and the Panglossian paradigm: A critique of the adaptationist programme. *Proceedings of the Royal Society B 205,* 581–598.

21. Holland, J. H. (1992). *Adaptation in natural and artificial systems: An introductory analysis with applications to biology, control, and artificial intelligence* (2nd ed.). Cambridge, MA: MIT Press/Bradford Books.

22. Holland, J. H. (1995). *Hidden order: How adaptation builds complexity*. Reading, MA: Addison-Wesley/Helix Books.

23. Kimura, M. (1983). *The neutral theory of molecular evolution*. Cambridge, U.K.: Cambridge University Press.

24. Lindgren, K. (1992). Evolutionary phenomena in simple dynamics. In C. G. Langton, C. Taylor, D. Farmer, & S. Rasmussen (Eds.), *Artificial Life II, Santa Fe Institute Studies in the Sciences of Complexity* (pp. 295–312). Redwood City, CA: Addison-Wesley.

25. Maley, C. C. (1994). The computational completeness of Ray's Tierran assembly language. In C. G. Langton (Ed.), *Artificial Life III, Santa Fe Institute Studies in the Sciences of Complexity* (pp. 503–514). Redwood City, CA: Addison-Wesley.

26. Maynard Smith, J. (1975). *The theory of evolution* (3rd ed.). New York: Penguin.

27. Mayr, E. (1988). *Towards a new philosophy of biology*. Cambridge, MA: Harvard University Press.

28. Packard, N. H. (1989). Intrinsic adaptation in a simple model for evolution. In C. G. Langton (Ed.), *Artificial Life, Sante Fe Institute Studies in the Sciences of Complexity* (pp. 141–155). Redwood City, CA: Addison-Wesley.

29. Palmer, R. G., Arthur, W. B., Holland, J. H., LeBaron, B., & Taylor, P. (1994). Artificial economic life: A simple model of a stock market. *Physica D, 75*, 264–274.

30. Ray, T. S. (1992). An approach to the synthesis of life. In C. G. Langton, C. Taylor, D. Farmer, & S. Rasmussen (Eds.), *Artificial Life II, Santa Fe Institute Studies in the Sciences of Complexity* (pp. 371–408). Redwood City, CA: Addison-Wesley.

31. Ray, T. S. (1994). An evolutionary approach to synthetic biology: Zen and the art of creating life. *Artificial Life, 1*, 179–209.

32. Ray, T. S. (1994). Evolution, complexity, entropy, and artificial reality. *Physica D, 75*, 239–263.

33. Ray, T. S. (1994). Evolution and complexity. In G. A. Cowan, D. Pines, & D. Metzger (Eds.), *Complexity: Metaphors, models, and reality* (pp. 161–173). Redwood City, CA: Addison-Wesley.

34. Ray, T. S. (1995). Artificial life and the evolution of distributed processes. *Journal of Japanese Society for Artificial Intelligence, 10*, 213–221.

35. Ray, T. S. (1996). Software evolution. *Systems, Control and Information, 40*, 337–343.

36. Sepkoski, J. J., Jr. (1992). *A compendium of fossil marine animal families* (2nd ed.). Milwaukee Public Museum Contributions in Biology and Geology, no. 83.

37. Thearling, K., & Ray, T. (1994). Evolving multi-cellular artificial life. In R. Brooks & P. Maes (Eds.), *Artificial Life IV* (pp. 283–288). Cambridge, MA: MIT Press/Bradford Books.

38. West-Eberhard, M. J. (1992). Adaptation: Current uses. In E. F. Keller & E. A. Lloyd (Eds.), *Keywords in evolutionary biology* (pp. 13–18). Cambridge, MA: Harvard University Press.